

# Anthropogenic Decline in High-Latitude Ocean Carbonate by 2100

James C. Orr<sup>1</sup>, Victoria J. Fabry<sup>2</sup>, Olivier Aumont<sup>1\*</sup>, Laurent Bopp<sup>1</sup>, Scott C. Doney<sup>3</sup>, Richard M. Feely<sup>4</sup>, Anand Gnanadesikan<sup>5</sup>, Nicolas Gruber<sup>6</sup>, Akio Ishida<sup>7</sup>, Fortunat Joos<sup>8</sup>, Robert M. Key<sup>9</sup>, Keith Lindsay<sup>10</sup>, Ernst Maier-Reimer<sup>11</sup>, Richard Matear<sup>12</sup>, Patrick Monfray<sup>1†</sup>, Anne Mouchet<sup>13</sup>, Raymond G. Najjar<sup>14</sup>, Gian-Kasper Plattner<sup>8</sup>, Keith B. Rodgers<sup>1\*</sup>, Christopher L. Sabine<sup>4</sup>, Jorge L. Sarmiento<sup>9</sup>, Reiner Schlitzer<sup>15</sup>, Richard D. Slater<sup>9</sup>, Ian J. Totterdell<sup>16</sup>, Marie-France Weirig<sup>15</sup>, Yasuhiro Yamanaka<sup>7</sup>, & Andrew Yool<sup>16</sup>

<sup>1</sup>*LSCE, UMR CEA-CNRS, CEA Saclay, F-91191 Gif-sur-Yvette, France*

<sup>2</sup>*Dept. of Biol. Sciences, Cal. State University San Marcos, San Marcos, CA 92096–0001, USA*

<sup>3</sup>*WHOI, Woods Hole, MA 02543-1543, USA.*

<sup>4</sup>*PMEL/NOAA Seattle, WA 98115-6349, USA.*

<sup>5</sup>*NOAA/GFDL, Princeton, NJ 08542, USA.*

<sup>6</sup>*IGPP, UCLA, Los Angeles, CA 90095-4996, USA.*

<sup>7</sup>*Frontier Research Center for Global Change, Yokohama 236-0001, Japan.*

<sup>8</sup>*Climate and Environmental Physics, University of Bern, CH-3012 Bern, Switzerland.*

<sup>9</sup>*AOS Program, Princeton University, Princeton, NJ 08544-0710, USA*

<sup>10</sup>*NCAR, Boulder, CO 80307-3000, USA.*

<sup>11</sup>*Max Planck Institut für Meteorologie, D-20146 Hamburg, Germany.*

<sup>12</sup>*CSIRO Division of Marine Research, Hobart, TAS 7001, Australia.*

<sup>13</sup>*Astrophysics & Geophysics Institute, University of Liege, B-4000 Liege, Belgium.*

<sup>14</sup>*Dept. of Meteorology, Penn. State University, University Park, PA 16802-5013, USA.*

<sup>15</sup>*Alfred Wegener Institute for Polar and Marine Research, D-27515 Bremerhaven, Germany.*

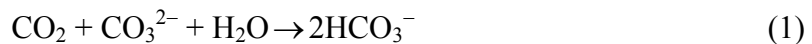
<sup>16</sup>*Southampton Oceanography Centre, Southampton SO14 3ZH, UK.*

\*Present address: LOCEAN, 4 Place Jussieu, F-75252 Paris cedex 05, France

†Present address: LEGOS, UMR 5566 CNES-CNRS-IRD-UPS, F-31401 Toulouse, France.

**The surface ocean is everywhere saturated with respect to calcium carbonate (CaCO<sub>3</sub>). Yet increasing atmospheric CO<sub>2</sub> reduces ocean pH and carbonate ion concentrations [CO<sub>3</sub><sup>2-</sup>] and thus the level of saturation. Reduced saturation states are expected to affect marine calcifiers even though it has been estimated that all surface waters will remain saturated for centuries. Here we show, however, that some surface waters will become undersaturated within decades. When atmospheric CO<sub>2</sub> reaches 550 ppmv, in year 2050 under the IS92a business-as-usual scenario, Southern Ocean surface waters begin to become undersaturated with respect to aragonite, a metastable form of CaCO<sub>3</sub>. By 2100 as atmospheric CO<sub>2</sub> reaches 788 ppmv, undersaturation extends throughout the entire Southern Ocean (< 60°S) and into the subarctic Pacific. These changes will threaten high-latitude aragonite secreting organisms including cold-water corals, which provide essential fish habitat, and shelled pteropods, an abundant food source for marine predators.**

Ocean uptake of CO<sub>2</sub> will help moderate future climate change but the associated chemistry, namely hydrolysis of CO<sub>2</sub> in seawater, increases the hydrogen ion concentration [H<sup>+</sup>]. Surface ocean pH is already 0.1 unit lower than preindustrial values. By the end of the century it will probably become another 0.3 to 0.4 units lower<sup>1,2</sup>, meaning [H<sup>+</sup>] will increase by 100 to 150%. Simultaneously, the aqueous CO<sub>2</sub> concentration [CO<sub>2</sub>(aq)] will increase and [CO<sub>3</sub><sup>2-</sup>] will decrease, making it harder for marine calcifying organisms to form biogenic CaCO<sub>3</sub>. Substantial experimental evidence indicates that calcification rates will decrease in low latitude corals<sup>3-5</sup>, which form reefs out of aragonite, and in phytoplankton that form their tests (shells) out of calcite<sup>6,7</sup>, the stable form of CaCO<sub>3</sub>. Calcification rates will decline along with [CO<sub>3</sub><sup>2-</sup>] due to its reaction with increasing concentrations of anthropogenic CO<sub>2</sub>



even though surface waters remain supersaturated with respect to CaCO<sub>3</sub>, a condition that previous studies have predicted will persist for hundreds of years<sup>8,4,9</sup>.

Recent predictions of future changes in surface ocean pH and carbonate chemistry have largely focused on global average conditions<sup>1,2,10</sup> or on the low latitudes<sup>4</sup>, where reef building corals are abundant. Here we focus on future surface and subsurface changes in high latitude regions where planktonic shelled pteropods are prominent components of the upper ocean biota in the Southern Ocean, Arctic Ocean, and subarctic Pacific<sup>11-15</sup>. Recently, it has been suggested that the cold surface waters in such regions will begin to become undersaturated with respect to aragonite only when atmospheric CO<sub>2</sub> reaches 1200 ppmv, more than 4 times the preindustrial level (4×CO<sub>2</sub>) of 280 ppmv<sup>9</sup>. In contrast, our results suggest that some polar and subpolar surface waters will become undersaturated at ~ 2×CO<sub>2</sub>, i.e., probably within the next 50 years.

### **Changes in Carbonate**

We have computed modern ocean carbonate chemistry from observed alkalinity and dissolved inorganic carbon (DIC), relying on data collected during the CO<sub>2</sub> Survey of the World Ocean Circulation Experiment (WOCE) and the Joint Global Ocean Flux Study (JGOFS). These observations are centred around 1994, and have recently been provided as a global-scale, gridded data product GLODAP<sup>16</sup> (see Supplementary Information). Modern surface [CO<sub>3</sub><sup>2-</sup>] varies meridionally by more than a factor of two, from average Southern Ocean concentrations of 105 μmol kg<sup>-1</sup> to average tropical concentrations of 240 μmol kg<sup>-1</sup> (Fig. 1). Low Southern Ocean [CO<sub>3</sub><sup>2-</sup>] is due to (1) low surface temperatures and carbonate thermodynamics (high solubility) as well as (2) large local amounts of upwelled deep water, which contain high [CO<sub>2</sub>(aq)] from organic matter remineralisation. These two effects reinforce one another, yielding a high positive correlation of present-day [CO<sub>3</sub><sup>2-</sup>] with temperature (e.g., R<sup>2</sup> = 0.92 for annual mean surface maps). Changes in [CO<sub>3</sub><sup>2-</sup>] and [CO<sub>2</sub>(aq)] are also inextricably linked to changes in other carbonate chemistry variables (Fig. S1).

We also estimated preindustrial [CO<sub>3</sub><sup>2-</sup>] from the same data, after subtracting data-based estimates of anthropogenic DIC<sup>17</sup> from the modern DIC observations and assuming that preindustrial and modern alkalinity fields were identical (see Supplementary Information). Relative to preindustrial conditions, invasion of anthropogenic CO<sub>2</sub> has already reduced modern surface [CO<sub>3</sub><sup>2-</sup>] by more than 10%, i.e., by 29 μmol kg<sup>-1</sup> in the tropics and 18 μmol kg<sup>-1</sup> in the Southern Ocean. Nearly identical results were found when instead of the data-based anthropogenic CO<sub>2</sub> estimates, we used simulated anthropogenic CO<sub>2</sub>, i.e., the median from 13 models that participated in the second phase of the Ocean Carbon-Cycle Model Intercomparison Project, OCMIP-2 (Fig. 1c).

To quantify future changes in carbonate chemistry we used simulated DIC from ocean models that were forced by two atmospheric CO<sub>2</sub> scenarios: the continually

increasing IPCC IS92a scenario (788 ppmv in 2100) and the IPCC S650 stabilisation scenario (563 ppmv in 2100) (Fig. 1). Simulated perturbations in DIC relative to 1994 (the GLODAP reference year), were added to the modern DIC data; again, alkalinity was assumed constant. To provide a measure of uncertainty we report model results as the OCMIP median  $\pm 2\sigma$ . The median generally outperformed individual models in OCMIP model-data comparison (Fig. S2). By year 2100 as atmospheric CO<sub>2</sub> reaches 788 ppmv under the IS92a scenario, average tropical surface [CO<sub>3</sub><sup>2-</sup>] declines to  $149 \pm 14 \mu\text{mol kg}^{-1}$ . This is a 45% reduction relative to the preindustrial ocean, in agreement with previous predictions<sup>8,4</sup>. In the Southern Ocean, surface concentrations dip to  $55 \pm 5 \mu\text{mol kg}^{-1}$ , i.e., 18% below the threshold where aragonite becomes undersaturated ( $66 \mu\text{mol kg}^{-1}$ ).

These changes extend well below the sea surface. Throughout the Southern Ocean (all waters south of 60°S), the entire water column becomes undersaturated with respect to aragonite. During the 21st century under IS92a, the Southern Ocean's aragonite saturation horizon (the limit between undersaturation and supersaturation) shoals from its present average depth of 730 m (Fig. S3) all the way to the surface (Fig. 2). Simultaneously, in a portion of the subarctic Pacific, the aragonite saturation horizon shoals from depths of about 120 m to the surface. In the North Atlantic, surface waters remain saturated with respect to aragonite, but the aragonite saturation horizon shoals dramatically, e.g., from 2600 m to 115 m north of 50°N. The greater erosion in the North Atlantic is due to deeper penetration and higher concentrations of anthropogenic CO<sub>2</sub>, a tendency that is already evident in present-day data-based estimates<sup>18,17</sup> and in models<sup>19,20</sup> (Figs. S4 and S5). Less spectacular changes were found for the calcite saturation horizon. For example, in 2100 the average calcite saturation horizon in the Southern Ocean stays below 2200 m. Nonetheless, in 2100 Weddell Sea surface waters become slightly undersaturated with respect to calcite.

In the more conservative S650 scenario, the atmosphere reaches  $2\times\text{CO}_2$  in 2100, 50 years later than with the IS92a scenario. In 2100, average Southern Ocean surface waters remain slightly supersaturated with respect to aragonite. But the models also simulate that the Southern Ocean's average aragonite saturation horizon will have shoaled from 730 m to 60 m and that the entire water column in the Weddell Sea will have become undersaturated (Fig. 2). In the north, all surface waters remain saturated under the S650 scenario. North of  $50^\circ\text{N}$ , the annual average, aragonite saturation horizon shoals from 140 m to 70 m in the Pacific, whereas it shoals by 2000 m to 610 m in the North Atlantic. Therefore under either scenario, the OCMIP models simulated large changes in surface and subsurface  $[\text{CO}_3^{2-}]$ . Yet these models account for only the direct geochemical effect of increasing atmospheric  $\text{CO}_2$  because they were all forced with prescribed modern climate conditions.

In addition to this direct geochemical effect, ocean  $[\text{CO}_3^{2-}]$  is also altered by climate variability and climate change. To quantify the added effect of future climate change, we analysed results from three atmosphere-ocean climate models that each included an ocean carbon cycle component (see Supplementary Information). These three models agree that 21st century climate change will cause a general increase in surface ocean  $[\text{CO}_3^{2-}]$  (Fig. 3), mainly because most surface waters will be warmer. Moreover, the models agree that the magnitude of this increase in  $[\text{CO}_3^{2-}]$  is small, typically counteracting less than 10% of the decrease due to the geochemical effect. High-latitude surface waters show the smallest increases in  $[\text{CO}_3^{2-}]$ , even small reductions in some cases. Therefore, our analysis suggests that physical climate change alone will not substantially alter high-latitude surface  $[\text{CO}_3^{2-}]$  during the 21st century.

Climate also varies seasonally and interannually, whereas our previous focus has been on annual changes. To illustrate how climate variability affects surface  $[\text{CO}_3^{2-}]$ , we used results from an ocean carbon cycle model forced with the daily NCEP

reanalysis fields<sup>21</sup> over 1948-2003 (see Supplementary Information). These fields are observationally based and vary on seasonal and interannual time scales. Simulated interannual variability in surface ocean  $[\text{CO}_3^{2-}]$  is negligible when compared with the magnitude of the anthropogenic decline (Fig. 3b). Seasonal variability is also negligible except in the high latitudes, where surface  $[\text{CO}_3^{2-}]$  varies by about  $\pm 15 \mu\text{mol kg}^{-1}$  when averaged over large regions. This is smaller than the 21st century's transient change (e.g.,  $\sim 50 \mu\text{mol kg}^{-1}$  in the Southern Ocean). However, high-latitude surface waters do become substantially less saturated during winter, because of cooling (higher  $[\text{CO}_2(\text{aq})]$ ) and greater upwelling of DIC-enriched deep water, in agreement with previous observations in the North Pacific<sup>22</sup>. Thus high-latitude undersaturation will be first reached during winter.

Our predicted changes may be compared to those found in earlier studies, which focused on surface waters in the tropics<sup>8</sup> and in the subarctic Pacific<sup>23,22</sup>. These studies assumed thermodynamic equilibrium between  $\text{CO}_2$  in the atmosphere and surface waters at their in situ alkalinity, temperature, and salinity. If the  $\text{pCO}_2$  in the equilibrium approach is taken only to represent seawater  $\text{pCO}_2$ , then results agree with our non-equilibrium approach, when the sets of carbonate chemistry constants are identical (Fig. 4). However, assuming equilibrium with the atmosphere leads to the prediction that future undersaturation will occur too soon (at lower atmospheric  $\text{CO}_2$ ), mainly because the anthropogenic transient in the ocean actually lags that in the atmosphere. For example, with the equilibrium approach we predict that average surface waters in the Southern Ocean become undersaturated when atmospheric  $\text{pCO}_2$  is 550 ppmv (year 2050 under IS92a), whereas our non-equilibrium approach that uses models and data indicates that such will occur at 635 ppmv (year 2070). Despite these differences, both approaches indicate that the Southern Ocean surface waters will probably become undersaturated with respect to aragonite during this century. Conversely, both these approaches disagree with a recent assessment<sup>9</sup> that used a variant of the standard

thermodynamic equilibrium approach, where an incorrect input temperature was used inadvertently.

## Uncertainties

The three coupled climate-carbon models show little effect of climate change on surface  $[\text{CO}_3^{2-}]$  (Fig. 3a vs. Fig. 1) partly because air-sea  $\text{CO}_2$  exchange largely compensates for changes in surface DIC caused by changes in marine productivity and circulation. In subsurface waters where such compensation is lacking, these models could under- or over-predict the extent to which  $[\text{CO}_3^{2-}]$  will change as a result of changes in overlying marine productivity (see Supplementary Information). However, we are confident in the model-predicted trend, which only worsens the decline in subsurface  $[\text{CO}_3^{2-}]$ . That is, all coupled climate models predict a more vigorous hydrological cycle with increased evaporation in the tropics and increased precipitation in the high latitudes<sup>24</sup>. Increased high-latitude precipitation drives freshening of surface waters and thus greater vertical stratification. This leads to a decrease in high-latitude nutrients, but an increase in light availability. The latter wins out in the Southern Ocean of the IPSL-Paris model so that at  $2\times\text{CO}_2$  there is a 10% increase in local surface carbon export of particulate organic carbon (POC)<sup>25</sup>. Subsequent remineralisation of this exported POC within the thermocline leads to increased DIC, which only exacerbates the decrease in high-latitude subsurface  $[\text{CO}_3^{2-}]$ .

The largest uncertainty by far, and the only means to limit the future decline in ocean  $[\text{CO}_3^{2-}]$ , is the atmospheric  $\text{CO}_2$  trajectory. To better characterise uncertainty due to  $\text{CO}_2$  emissions, we compared the six illustrative IPCC SRES scenarios in the reduced complexity, PIUB-Bern model. Under the moderate SRES B2 scenario, average Southern Ocean surface waters in that model become undersaturated with respect to aragonite when atmospheric  $\text{CO}_2$  reaches 600 ppmv in 2100 (Fig. 5). For the three higher emission SRES scenarios (A1FI, A2, A1B), these waters become undersaturated



sooner (between 2058 and 2073); for the two lower emission scenarios (A1T, B1), these waters remain slightly supersaturated in 2100. Thus if atmospheric CO<sub>2</sub> rises above 600 ppmv, most Southern Ocean surface waters will become undersaturated with respect to aragonite. Yet even below this level, the Southern Ocean's aragonite saturation horizon will shoal substantially (Fig. 2). For a given atmospheric CO<sub>2</sub> scenario, predicted changes in surface ocean [CO<sub>3</sub><sup>2-</sup>] are much more certain than are related changes in climate. The latter depend not only on the model response to CO<sub>2</sub> forcing but also on poorly constrained physical processes, such as those associated with clouds.

### **Ocean CO<sub>2</sub> Uptake**

With higher levels of anthropogenic CO<sub>2</sub> and lower surface [CO<sub>3</sub><sup>2-</sup>], the change in surface ocean DIC per unit change in atmospheric CO<sub>2</sub> (μmol kg<sup>-1</sup> per ppmv) will be about 60% lower in 2100 (under IS92a) than it is today. Simultaneously, the CO<sub>3</sub><sup>2-</sup>/CO<sub>2</sub>(aq) ratio will decrease from 4:1 to 1:1 in the Southern Ocean (Fig. 4). These decreases are due to the well-understood anthropogenic reduction in buffer capacity<sup>26</sup>, already accounted for in ocean carbon cycle models.

On the other hand, reduced export of CaCO<sub>3</sub> from the high latitudes would increase surface [CO<sub>3</sub><sup>2-</sup>], thereby increasing ocean CO<sub>2</sub> uptake and decreasing atmospheric CO<sub>2</sub>. Due to this effect, ocean CO<sub>2</sub> uptake could increase by 6 to 13 Pg C over the 21st century, based on one recent model study<sup>27</sup> that incorporated an empirical, CO<sub>2</sub>-dependant relationship for calcification<sup>7</sup>. Rates of calcification could decline even further, to zero, if waters actually became undersaturated with respect to both aragonite and calcite. We estimate that the total shutdown of high-latitude aragonite production would lead to at most a 0.25 Pg C yr<sup>-1</sup> increase in ocean CO<sub>2</sub> uptake, assuming that 1 Pg C yr<sup>-1</sup> of CaCO<sub>3</sub> is exported globally<sup>28</sup>, that up to half of that is aragonite<sup>29,9</sup>, and that perhaps half of all aragonite is exported from the high latitudes. The actual increase in ocean CO<sub>2</sub> uptake could be much lower because the aragonite fraction of the CaCO<sub>3</sub>

may be only 0.1 based on low-latitude sediment traps<sup>30</sup>, and the latitudinal distribution of aragonite export is uncertain. Thus increased CO<sub>2</sub> uptake from reduced export of aragonite will provide little compensation for decreases in ocean CO<sub>2</sub> uptake due to reductions in buffer capacity. Of greater concern are potential biological impacts due to future undersaturation.

### **Biological Impacts**

The changes in seawater chemistry that we project to occur during this century could have severe consequences for calcifying organisms, particularly shelled pteropods, the major planktonic producers of aragonite. Pteropod population densities are high in polar and subpolar waters. Yet only 5 species typically occur in such cold water regions and, of these, only 1-2 species are common at the highest latitudes<sup>31</sup>. High-latitude pteropods have 1-2 generations per year<sup>12,15,32</sup>, form integral components of food webs, and are typically found in the upper 300 m where they may reach densities of 100's to 1000's of individuals per m<sup>3</sup> (refs. 11,13-15). In the Ross Sea, for example, the prominent subpolar-polar pteropod *Limacina helicina* sometimes replaces krill as the dominant zooplankton and is considered an overall indicator of ecosystem health<sup>33</sup>. In the strongly seasonal high latitudes, sedimentation pulses of pteropods frequently occur just after summer<sup>15,34</sup>. In the Ross Sea, pteropods account for the majority of the annual export flux of both carbonate and organic carbon<sup>35,34</sup>. South of the Antarctic Polar Front pteropods also dominate the export flux of CaCO<sub>3</sub><sup>36</sup>.

Pteropods may be unable to maintain shells in waters that are undersaturated with respect to aragonite. Data from sediment traps indicate that empty pteropod shells exhibit pitting and partial dissolution as soon as they fall below the aragonite saturation horizon<sup>37,22,36</sup>. In vitro measurements confirm such rapid pteropod shell dissolution rates<sup>38</sup>. New experimental evidence suggests that even shells of live pteropods dissolve rapidly once surface waters become undersaturated with respect to aragonite<sup>9</sup>. Here we

show that when the live subarctic pteropod *Clio pyramidata* is subjected to undersaturation, similar to what we predict for Southern Ocean surface waters in 2100 under IS92a, marked dissolution occurs within 48 hours at the growing edge of the shell aperture (Fig. 6). Etch pits formed on the shell surface at the apertural margin, which is typically  $\sim 7 \mu\text{m}$  thick, as the  $< 1\text{-}\mu\text{m}$  exterior (prismatic layer) peeled back (Fig. 6c), exposing the underlying aragonitic rods to dissolution. Fourteen individuals were tested. All of them showed similar dissolution along their growing edge, even though they all remained alive. If *C. pyramidata* cannot grow its protective shell, we would not expect it to survive in waters that become undersaturated with respect to aragonite.

If the response of other high latitude pteropod species to aragonite undersaturation is similar to that of *C. pyramidata*, we hypothesise that these pteropods will not be able to adapt quickly enough to live in the undersaturated conditions that will occur over much of the high-latitude surface ocean during the 21st century. Their distributional ranges would then be reduced, both within the water column, disrupting vertical migration patterns, and latitudinally, imposing a shift towards lower latitude surface waters that remain supersaturated with respect to aragonite. At present, we do not know if pteropod species endemic to polar regions could disappear altogether or if they can make the transition to live in warmer, carbonate-rich waters at lower latitudes under a different ecosystem. If pteropods are excluded from polar and subpolar regions, their predators will be affected immediately. For instance, gymnosomes are zooplankton that feed exclusively on shelled pteropods<sup>39,33</sup>. Pteropods also contribute to the diet of diverse carnivorous zooplankton, mytophid and notothenoid fishes<sup>40-42</sup>, North Pacific salmon<sup>43,44</sup>, mackerel, herring, cod, and baleen whales<sup>45</sup>.

Surface dwelling calcitic plankton such as foraminifera and coccolithophorids, may fare better temporarily. However, the beginnings of high-latitude calcite undersaturation will only lag that for aragonite by 50 to 100 years. The diverse benthic

calcareous organisms in high-latitude regions may also be threatened, including cold-water corals which provide essential fish habitat<sup>46</sup>. Cold-water corals appear much less abundant in the North Pacific than in the North Atlantic<sup>46</sup>, where the aragonite saturation horizon is much deeper (Fig. 2). Moreover, some important taxa in Arctic and Antarctic benthic communities secrete magnesian calcite, which can be more soluble than aragonite. These include gorgonians<sup>46</sup>, coralline red algae, and echinoderms (sea urchins)<sup>47</sup>. At  $2\times\text{CO}_2$ , juvenile echinoderms stopped growing and produced more brittle and fragile exoskeletons in a subtropical 6-month manipulative experiment<sup>48</sup>. For high latitude calcifiers though, responses to reduced  $[\text{CO}_3^{2-}]$  have generally not been studied. Yet experimental evidence from lower latitude, shallow dwelling calcifiers reveals a reduced ability to calcify with decreasing carbonate saturation state<sup>9</sup>. Given that at  $2\times\text{CO}_2$ , calcification rates in some shallow dwelling calcareous organisms may decline by up to 50%<sup>9</sup>, some calcifiers could have difficulty surviving even long enough to experience undersaturation. Certainly, they have not experienced undersaturation for at least the last 400,000 years<sup>49</sup> and probably much longer<sup>50</sup>.

Changes in high-latitude seawater chemistry that will occur by the end of the century could well alter the structure and biodiversity of polar ecosystems, impacting multiple trophic levels. Assessing these impacts is impeded by the scarcity of relevant data.

Figure 1: Increasing atmospheric  $\text{CO}_2$  and decreasing surface ocean pH and  $[\text{CO}_3^{2-}]$ . **a** Atmospheric  $\text{CO}_2$  used to force 13 OCMIP models over the industrial period and for two future scenarios: IS92a (I) and S650 (S). Increases in atmospheric  $\text{CO}_2$  lead to reductions in **b** surface ocean pH and **c** surface ocean  $[\text{CO}_3^{2-}]$  ( $\mu\text{mol kg}^{-1}$ ). Results are given as global zonal averages for the 1994 data and the preindustrial ocean. The latter were obtained by subtracting data-based anthropogenic DIC<sup>17</sup> (solid) as well as by subtracting model-based

anthropogenic DIC (OCMIP median, dotted line; OCMIP range, grey shading). Future results come from the 1994 data plus the simulated DIC perturbations to 2100 for the two scenarios; results are also shown for 2300 with S650 (thick dashed line). The small effect of future climate change simulated by the IPSL climate-carbon model is added as a perturbation to IS92a in 2100 (thick dotted line); two other climate-carbon models (PIUB-Bern and CSIRO) show similar results (Fig. 3a). The thin dashed lines indicating the  $[\text{CO}_3^{2-}]$  for seawater in equilibrium with aragonite and calcite are nearly flat, revealing weak temperature sensitivity.

Figure 2: The aragonite saturation state in 2100 as indicated by  $\Delta[\text{CO}_3^{2-}]_A$ . The  $\Delta[\text{CO}_3^{2-}]_A$  is the in situ  $[\text{CO}_3^{2-}]$  minus that for aragonite equilibrated seawater at the same salinity, temperature, and pressure. Shown are the OCMIP-2 median concentrations ( $\mu\text{mol kg}^{-1}$ ) in year 2100 under scenario IS92a: **a** surface map; **b** Atlantic and **c** Pacific zonal averages. Thick lines indicate the aragonite saturation horizon in 1765 (white dashes), 1994 (white solid), and 2100 (black solid for S650 [S]; black dashes for IS92a [I]). Positive  $\Delta[\text{CO}_3^{2-}]_A$  indicates supersaturation; negative  $\Delta[\text{CO}_3^{2-}]_A$  indicates undersaturation.

Figure 3: Climate-induced changes in surface  $[\text{CO}_3^{2-}]$ . **a** The 21st century shift in zonal mean surface ocean  $[\text{CO}_3^{2-}]$  due only to climate change, from three atmosphere-ocean climate models (CSIRO-Hobart, IPSL-Paris, and PIUB-Bern) that each include an ocean carbon cycle component (see Supplementary Information). **b** The regional-scale seasonal and interannual variability as simulated by an ocean carbon cycle model forced with reanalysed climate forcing.

Figure 4: Key surface carbonate chemistry variables as a function of  $\text{pCO}_2$  ( $\mu\text{atm}$ ). Shown are both  $[\text{CO}_3^{2-}]$  (solid) and  $[\text{CO}_2(\text{aq})]$  (dashed) for

average surface waters in the tropical ocean (thick), the Southern Ocean (thickest) and the global ocean (thin). Solid and dashed lines are calculated from the thermodynamic equilibrium approach. For comparison, open symbols are for  $[\text{CO}_3^{2-}]$  from our non-equilibrium, model-data approach vs. seawater  $\text{pCO}_2$  (circles) and atmospheric  $\text{pCO}_2$  (squares); symbol thickness corresponds with line thickness, which indicates the regions for area-weighted averages. The nearly flat, thin dotted lines indicate the  $[\text{CO}_3^{2-}]$  for seawater in equilibrium with aragonite and calcite.

Figure 5: Time series of average surface  $[\text{CO}_3^{2-}]$  in the Southern Ocean for the PIUB-Bern reduced complexity model (see Fig. 3 and Supplementary Information) under the six illustrative IPCC SRES scenarios. The results for the SRES scenarios A1T and A2 are similar to those for the non-SRES scenarios S650 and IS92a, respectively.

Figure 6: Shell from a live pteropod, *Clio pyramidata*, collected from the subarctic Pacific and kept in water undersaturated with respect to aragonite for 48 hours. The **a** whole shell has superimposed white rectangles that indicate the three corresponding magnified areas: **b** shell surface, which reveals etch pits from dissolution and resulting exposure of aragonitic rods; **c** prismatic layer, which has begun to peel back, increasing the surface area over which dissolution occurs; and **d** aperture region, which reveals advanced shell dissolution when compared to **e** a typical *C. pyramidata* shell not exposed to undersaturated conditions.

## References

1. Haugan, P. M. & Drange, H. Effects of  $\text{CO}_2$  on the ocean environment. *Energy Convers. Mgmt.* **37**, 1019-1022 (1996).

2. Brewer, P. G. Ocean chemistry of the fossil fuel CO<sub>2</sub> signal: the haline signal of "business as usual". *Geophys. Res. Lett.* **24**, 1367-1369 (1997).
3. Gattuso, J.-P., Frankignoulle, M., Bourge, I., Romaine, S. & Buddemeier, R. W. Effect of calcium carbonate saturation of seawater on coral calcification. *Global and Planetary Change* **18**, 37-46 (1998).
4. Kleypas, J. A. *et al.* Geochemical consequences of increased atmospheric carbon dioxide on coral reefs. *Science* **284**, 118-120 (1999).
5. Langdon, C. *et al.* Effect of elevated CO<sub>2</sub> on the community metabolism of an experimental coral reef. *Global Biogeochem. Cycles* **17**, 1011, doi:10.1029/2002GB001941 (2003).
6. Riebesell, U. *et al.* Reduced calcification of marine plankton in response to increased atmospheric CO<sub>2</sub>. *Nature* **407**, 364-367 (2000).
7. Zondervan, I., Zeebe, R., Rost, B. & Riebesell, U. Decreasing marine biogenic calcification: A negative feedback on rising atmospheric pCO<sub>2</sub>. *Global Biogeochem. Cycles* **15**, 507-516 (2001).
8. Broecker, W. S. & Peng, T.-H. Fate of fossil fuel carbon dioxide and the global carbon budget. *Science* **206**, 409-418 (1979).
9. Feely, R. A. *et al.* The impact of anthropogenic CO<sub>2</sub> on the CaCO<sub>3</sub> system in the oceans. *Science* **305**, 362-366 (2004).
10. Caldeira, K. & Wickett, M. E. Anthropogenic carbon and ocean pH. *Science* **425**, 365 (2003).
11. Urban-Rich, J., Dagg, M. & Peterson, J. Copepod grazing on phytoplankton in the Pacific sector of the Antarctic Polar Front. *Deep-Sea Res.* **48**, 4223-4246 (2001).

12. Kobayashi, H. A. Growth cycle and related vertical distribution of the thecosomatous pteropod *Spiratella "Limacina" helicina* in the central Arctic Ocean. *Marine Biology* **26**, 295-301 (1974).
13. E. A. Pakhomov, H. M. V., Atkinson, A., Laubscher, R. K. & Taunton-Clark, J. Structure and grazing impact of the mesozooplankton community during late summer 1994 near South Georgia, Antarctica. *Polar Biology* **18**, 180-192 (1997).
14. Fabry, V. J. Aragonite production by pteropod molluscs in the subarctic Pacific. *Deep-Sea Res. I* **36**, 1735-1751 (1989).
15. Bathmann, U., Noji, T. T. & Bodungen, B. Sedimentation in the Norwegian Sea in autumn. *Deep-Sea Res.* **38**, 1341-1360 (1991).
16. Key, R. M. *et al.* A global ocean carbon climatology: Results from Global Data Analysis Project (GLODAP. *Global Biogeochem. Cycles* **18**, GB4031, doi:10.1029/2004GB002247 (2004).
17. Sabine, C. L. *et al.* The ocean sink for anthropogenic CO<sub>2</sub>. *Science* **305**, 367-370 (2004).
18. Gruber, N. Anthropogenic CO<sub>2</sub> in the Atlantic Ocean. *Global Biogeochem. Cycles* **12**, 165-191 (1998).
19. Sarmiento, J. L., Orr, J. C. & Siegenthaler, U. A perturbation simulation of CO<sub>2</sub> uptake in an ocean general circulation model. *J. Geophys. Res.* **97**, 3621-3645 (1992).
20. Orr, J. C. *et al.* Estimates of anthropogenic carbon uptake from four three-dimensional global ocean models. *Global Biogeochem. Cycles* **15**, 43-60 (2001).
21. Kalnay, E. *et al.* The NCEP/NCAR 40-year reanalysis project. *Bull. Am. Meteor. Soc.* **77**, 437-471 (1996).
22. Feely, R. A. *et al.* Winter-summer variations of calcite and aragonite saturation in the northeast Pacific. *Mar. Chem.* **25**, 227-241 (1988).



23. Feely, R. A., Byrne, R. H., Betzer, P. R., Gendron, J. F. & Acker, J. G. Factors influencing the degree of saturation of the surface and intermediate waters of the North Pacific Ocean with respect to aragonite. *J. Geophys. Res.* **89**, 10,631-10,640 (1984).
24. Sarmiento, J. L. *et al.* Response of ocean ecosystems to climate warming. *Global Biogeochem. Cycles* **18**, GB3003, doi:10.1029/2003GB002134 (2004).
25. Bopp, L. *et al.* Potential impact of climate change of marine export production. *Global Biogeochem. Cycles* **15**, 81-99 (2001).
26. Sarmiento, J. L., Le Quéré, C. & Pacala, S. Limiting future atmospheric carbon dioxide. *Global Biogeochem. Cycles* **9**, 121-137 (1995).
27. Heinze, C. Simulating oceanic CaCO<sub>3</sub> export production in the greenhouse. *Geophys. Res. Lett.* **31**, L16308, doi:10.1029/2004GL020613 (2004).
28. Iglesias-Rodriguez, M. D. *et al.* Representing key phytoplankton functional groups in ocean carbon cycle models: Coccolithophorids. *Global Biogeochem. Cycles* **16**, 1100, doi: 10.1029/2001GB00145 (2002).
29. Berner, R. A. Sedimentation and dissolution of pteropods in the ocean. In Andersen, N. R. & Malahoff, A. (eds.) *The Fate of Fossil Fuel CO<sub>2</sub> in the Oceans*, 243-260 (Plenum, New York, 1977).
30. Fabry, V. J. Shell growth rates of pteropod and heteropod molluscs and aragonite production in the open ocean: Implications for the marine carbonate system. *J. Mar. Res.* **48**, 209-222 (1990).
31. Bé, A. W. H. & Gilmer, R. W. A zoogeographic and taxonomic review of euthecosomatous Pteropoda. In Ramsey, A. (ed.) *Oceanic Micropaleontology*, vol. 1, 733-808 (Academic Press, London, 1977).

32. Dadon, J. R. & de Cidre, L. L. The reproductive cycle of the Thecomosomatous pteropod *Limacina retroversa* in the western South Atlantic. *Marine Biology* **114**, 439-442 (1992).
33. Seibel, B. A. & Dierssen, H. M. Cascading trophic impacts of reduced biomass in the Ross Sea, Antarctica: Just the tip of the iceberg? *Biol. Bull.* **205**, 93-97 (2003).
34. Accornero, A., Manno, C., Esposito, F. & M.C.Gambi. The vertical flux of particulate matter in the polyna of Terra Nova Bay. Part II. Biological components. *Antarctic Science* **15**, 175-188 (2003).
35. Collier, R., Dymond, J., Susumu Honjo, S. M., Francois, R. & Dunbar, R. The vertical flux of biogenic and lithogenic material in the Ross Sea: moored sediment trap observations 1996-1998. *Deep-Sea Res. II* **47**, 3491-3520 (2000).
36. Honjo, S., Francois, R., Manganini, S., Dymond, J. & Collier, R. Particle fluxes to the interior of the Southern Ocean in the western Pacific sector along 170°W. *Deep-Sea Res. II* **47**, 3521-3548 (2000).
37. Betzer, P. R., Byrne, R., Acker, J., Lewis, C. S. & Jolley, R. R. The oceanic carbonate system: a reassessment of biogenic controls. *Science* **226**, 1074-1077 (1984).
38. Byrne, R. H., Acker, J. G., Betzer, P. R., Feely, R. A. & Cates, M. H. Water column dissolution of aragonite in the Pacific Ocean. *Nature* **312**, 321-326 (1984).
39. Lalli, C. M. Structure and function of the buccal apparatus of *Clione limacina* (Phipps) with a review of feeding in gymnosomatous pteropods. *J. Exp. Mar. Biol. Ecol.* **4**, 101-118 (1970).
40. Foster, B. A. & Montgomery, J. C. Planktivory in benthic nototheniid fish in McMurdo Sound, Antarctica. *Environ. Biol. Fish.* **36**, 313-318 (1993).

41. Pakhovmov, E., Perissinotto, A. & McQuaid, C. D. Prey composition and daily rations of myctophid fishes in the Southern Ocean. *Marine Ecology Progress Series* **134**, 1-14 (1996).
42. La Mesa, M., Vacchi, M. & Sertorio, T. Z. Feeding plasticity of *Trematomus newnesi* (Pisces, Nototheniidae) in Terra Nova Bay, Ross Sea, in relation to environmental conditions. *Polar Biology* **23**, 38-45 (2000).
43. Willette, T. M. *et al.* Ecological processes influencing mortality of juvenile pink salmon (*Oncorhynchus gorbuscha*) in Prince William Sound, Alaska. *Fisheries Oceanography* **10**, 14-41 (2001).
44. Boldt, J. L. & Haldorson, L. J. Seasonal and geographical variation in juvenile pink salmon diets in the Northern Gulf of Alaska and Prince William Sound. *Transactions of the American Fisheries Society* **132**, 1035-1052 (2003).
45. Lalli, C. M. & Gilmer, R. *Pelagic Snails* (Stanford Univ. Press, Stanford, 1989).
46. Freiwald, A., Fosså, J. H., Grehan, A., Koslow, T. & Roberts, J. M. *Cold-water coral reefs: Out of sight no longer out of mind*. No. 22 in Biodiversity Series (UNEP-WCMC, Cambridge, UK, 2004).
47. Dayton, P. K. Polar benthos. In Smith, W. O. (ed.) *Polar Oceanography, Part B, Chemistry, Biology, and Geology*, 631-685 (Academic Press, San Diego, 1990).
48. Shirayama, Y. & Thornton, H. Effect of increased atmospheric CO<sub>2</sub> on shallow-water marine benthos. *J. Geophys. Res.* in press (2005).
49. Petit, J. R. *et al.* Climate and atmospheric history of the past 420,000 years from the Vostok ice core, Antarctica. *Nature* **399**, 429-436 (1999).
50. Pearson, P. N. & Palmer, M. R. Middle Eocene seawater pH and atmospheric carbon dioxide concentrations. *Science* **284**, 1824-1826 (1999).

**Supplementary Information** accompanies the paper on [www.nature.com/nature](http://www.nature.com/nature)

**Acknowledgements** We thank M. Gehlen for discussions and J.-M. Epitalon, P. Brockmann, and the Ferret developers for help with analysis. All but the climate simulations were made as part of the OCMIP project, which was launched in 1995 by the Global Analysis, Interpretation, and Modeling (GAIM) Task Force of the International Geosphere-Biosphere Program (IGBP) with funding from NASA. OCMIP-2 was supported by the EU GOSAC project and the U.S. JGOFS SMP funded through NASA. The interannual simulation was supported by the EU NOCES project, which is part of OCMIP-3.

**Competing Interests** The authors declare that they have no competing financial interests.

**Correspondence** Correspondence and requests for materials should be addressed to JCO (email: [orr@cea.fr](mailto:orr@cea.fr)).